JOURNAL OF CATALYSIS 136, 209–221 (1992)

Surface Structure and Reactivity of CrO_3/SiO_2 Catalysts

DU SOUNG KIM, JEAN-MICHEL TATIBOUET,* AND ISRAEL E. WACHS[1]

*Zettlemoyer Center for Surface Studies, Department of Chemical Engineering, Lehigh University, Bethlehem, Pennsylvania 18015; and *Laboratoire de Réactivité de Surface, U.R.A. 1106 CNRS, Université P. et M. Curie, 4 place Jussieu, 75252 Paris Cedex 05, France*

Received August 29, 1991; revised February 12, 1992

The molecular structure of the two-dimensional chromium oxide overlayer on the silica support at different chromium oxide contents has been investigated by *in situ* Raman spectroscopy. Under dehydrated conditions, the surface chromium oxide species on silica consists of a highly distorted, tetrahedral monochromate species regardless of chromium oxide content. The catalysts above 2% CrO_3/SiO_2 also contain crystalline α-Cr_2O_3 particles in addition to the surface monochromate species. The methanol oxidation studies reveal that the catalytic activity per Cr atom, the turnover number (TON), decreases as the chromium oxide content increases. The somewhat higher TON of the initial rate as compared to the steady state rate for the methanol oxidation reaction reflects the higher activity of the fully oxidized chromium oxide species relative to the partially reduced chromium oxide species for the methanol oxidation reaction. The major reaction product is HCHO, while $HCOOCH_3$, CO, and CO_2 are next in abundance. The selectivity for HCHO increases as the chromium oxide content increases and the precalcination temperature is increased. The opposite trend is observed for the selectivity of $HCOOCH_3$. These selectivity changes are due to dehydroxylization of the silica surface by precalcining at elevated temperatures and increasing the surface chromium oxide species. The current results suggest that HCHO and $HCOOCH_3$ are produced on two different catalytic sites: HCHO is formed on the Cr site, whereas $HCOOCH_3$ is produced via hemiacetal intermediates, which are formed by interaction between HCHO adsorbed on the Cr site and CH_3O adsorbed on the silica site. The CO and CO_2 combustion products are produced on both the Cr and silica site.

INTRODUCTION

Silica-supported chromium oxide is used as ethylene polymerization catalysts (Phillips process) in the petrochemical industry. The industrial importance of the CrO_3/SiO_2 system has motivated a large number of studies relating its specific surface properties (*1–7*) with catalytic behavior (*6, 8–11*). However, relatively few investigations have been devoted to the properties of CrO_3/SiO_2 catalysts for oxidation reactions (*12, 13*). At present, it is generally concluded that the silica support stabilizes the chromium(VI) oxide species, but there is still disagreement on the surface structures of the chromium oxide species on silica and the true nature of these species in the various catalytic processes (*1–2*).

The behavior of the Cr(VI) oxide species in aqueous solutions has been widely studied (*14–17*). The chromium oxide species present in aqueous solutions vary as functions of pH and the concentration of Cr(VI). At low chromium oxide concentrations under basic conditions, CrO_4^{2-} (monomers) species dominate, while at high concentrations under mild acidic conditions, $Cr_2O_7^{2-}$ (dimers) ions are the major species. In highly concentrated chromium oxide solutions under acidic conditions, $Cr_3O_{10}^{2-}$ (trimers) and $Cr_4O_{13}^{2-}$ (tetramers) species are also present. The aqueous impregnation process extensively hydroxylates the silica surface by hydrolyzing the Si–O–Si bonds. These surface hydroxyl groups, which can

[1] To whom correspondence should be addressed.

0021-9517/92 $5.00

be considered as in the case of the silicomolybdic acid–silica system (*18*) as a bidimensional solvent, are able to solvate the protons associated with the anionic species. Therefore, the structures of the chromium oxide species on the hydroxylated silica surface should not be very different from the species present in aqueous solutions (*4*). Raman spectroscopic studies have revealed that under hydrated conditions, chromium oxide monomers, dimers, trimers, and tetramers are present on the silica surface (*4*). Hardcastle and Wachs have demonstrated (*4*) that the surface structure under dehydrated conditions is quite different from that under hydrated conditions, and only monomeric chromium oxide species are present on the silica surface.

The surface morphology of heterogeneous catalysts can influence the catalytic activity and selectivity of partial oxidation reactions. For example, the methanol oxidation is well known as a reaction that is sensitive to the metal oxide structure (*19–22*), and it is used as a model reaction to characterize the surface properties of catalysts (*23–25*) as well as the interactions between the deposited surface oxide and the support (*26, 27*).

The objective of this study is to clarify the surface structure of the chromium oxide species on silica under dehydrated conditions and to elucidate the effects of surface properties on the catalytic activity and selectivity for methanol oxidation.

EXPERIMENTAL

Catalyst preparation. The silica-supported chromium oxide catalysts were prepared by the incipient wetness impregnation method with aqeous solutions of chromium nitrate ($Cr(NO_3)_3 \cdot 9H_2O$, Allied Chemical Co.). The support material used in this study was SiO_2 (Cab-O-Sil) with a surface area of ca. 300 $m^2\ g^{-1}$. After impregnation, the samples were subsequently dried at room temperature for 16 h, dried at 393 K for 16 h, and calcined at 773 K for 16 h.

Laser Raman spectroscopy. In situ Raman spectra of CrO_3/SiO_2 catalysts were obtained with a Spectra Physics Model 171 Ar^+ laser where the exciting line was typically 514.5 nm. The laser power at the sample was 10–20 mW. The scattered radiation was then directed into a Spex Triplemate Model 1877 spectrometer coupled to a Princeton Applied Research OMA III Model 1463 optical multichannel analyzer equipped with an intensified photodiode array detectors cooled thermoelectrically to 243 K. A modified version of the *in situ* cell developed by Wang (*28*) was used in all the *in situ* experiments. Prior to the measurement, the samples were dehydrated at 773 K for 1 h in flowing O_2 and the *in situ* Raman spectra were collected at room temperature. Ultrahigh-purity hydrocarbon-free oxygen (Linde gas) was purged through the cell during the acquisition of the Raman spectra.

Catalytic reactions. Partial oxidation of methanol was carried out in an isothermal fixed-bed continuous-flow reactor at atmospheric pressure and a temperature of 503 K. The reactor was held in a vertical position and made of a 6-mm-o.d. Pyrex glass tube, and the catalyst was held in between two layers of quartz wool. About 5–15 mg of catalyst sample was employed to obtain low conversions (below 5%). Prior to the reaction, the catalyst was typically treated with flowing O_2 at 573 K for 1 h, and then the temperature was reduced to the reaction temperature. The thermogravimetric analysis (TGA) study shows that the pretreatment conditions used in this study are sufficient for the formation of dehydrated chromium oxide species on SiO_2. The mixture gas, $CH_3OH/O_2/He$=6/11/83 (mol%), flowed from the top to the bottom of the reactor, and the reaction products were analyzed by an on-line gas chromatograph equipped with a FID and two TCD detector. The catalytic activity (TON) was calculated from the moles of methanol converted per mole of surface chromium atom per second. The catalytic activity and selectivity were measured at the steady state, which was reached

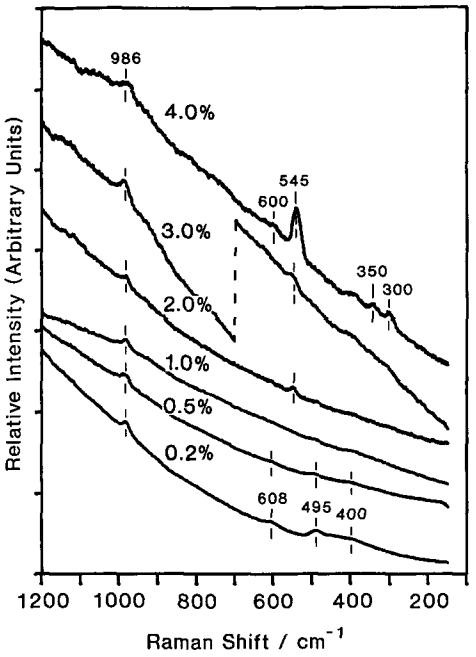

FIG. 1. *In situ* Raman spectra of CrO_3/SiO_2 catalysts as a function of chromium oxide content.

about 3 h after the initialization of the catalytic reaction.

RESULTS

Raman spectroscopy. The Raman spectra of the CrO_3/SiO_2 catalysts under dehydrated conditions, where the water molecules are desorbed from the surface, are shown in Fig. 1 as a function of chromium oxide content. The samples with low chromium oxide content possess the Raman bands which originate from the SiO_2 support as well as the surface chromium oxide species.The weak Raman bands observed at ~608, ~495, and ~400 cm^{-1} are characteristic Raman features of the silica support (*4*). The intensity of these bands decreases with increasing chromium oxide content since the silica surface is covered by the colored surface chromium oxide species. Only a single Raman band characteristic of the dehydrated surface chromium oxide species on the silica support is observed at ~986 cm^{-1} regardless of chromium oxide content. This band is assigned to the symmetric stretching mode of the terminal Cr=O bond of the dehydrated monomeric surface chromium oxide species on the silica support (*4, 28*). The presence of minor polymeric species such as dimers, trimers, and tetramers on the silica surface cannot be completely ruled out because the Raman spectra obtained in this study possess strong fluorescence from the background of the CrO_3/SiO_2 catalyst. The Raman band due to the crystalline α-Cr_2O_3 (*4*) is also observed at ~545 cm^{-1} for samples with at least 2% CrO_3, and the intensity of this band increases with further increase in chromium oxide content. In addition, the bands at ~600, ~350, and ~300 cm^{-1} for crystalline Cr_2O_3 are observed at higher chromium oxide content.

Methanol oxidation. The catalytic activity for methanol oxidation over the CrO_3/SiO_2 catalysts at different chromium oxide contents is shown in Figs. 2–4. The blank test of the SiO_2 support was performed under the same reaction conditions and only combustion products such as CO and CO_2 were observed. The catalytic activity (1

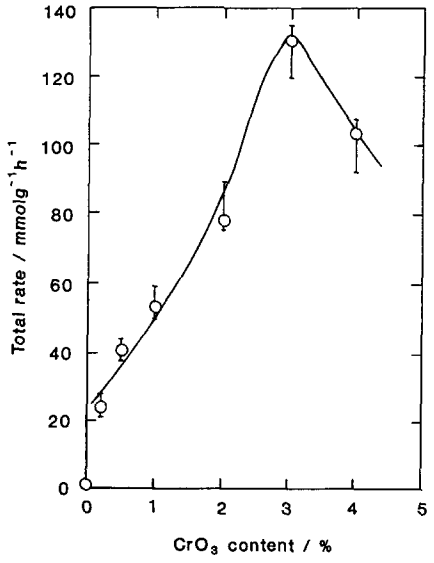

FIG. 2. The total rate of methanol oxidation at steady state over CrO_3/SiO_2 catalysts at different chromium oxide contents.

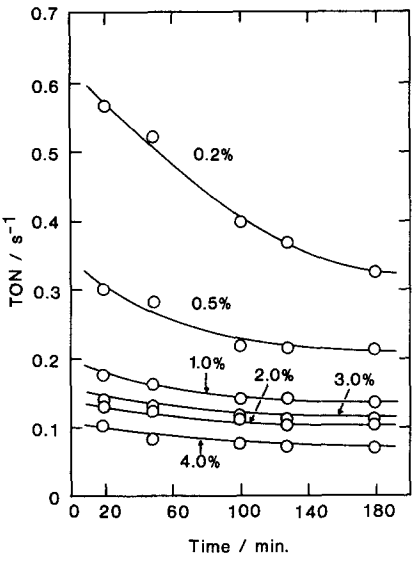

FIG. 3. The relation between TON and reaction time for the methanol oxidation over CrO_3/SiO_2 catalysts at different chromium oxide contents.

mmol g^{-1} h^{-1}) caused by the support itself is minimal in comparison to the supported chromium oxide catalysts (24–131 mmol g^{-1} h^{-1}) under the reaction conditions used in this study. As shown in Fig. 2, the overall activity (total rate) at steady state, expressed in millimoles of methanol converted per gram of catalyst per hour, is significantly enhanced by the addition of chromium oxide to the silica support and increases as the chromium oxide content increases up to 3% CrO_3. However, a decrease in the total rate is observed for the 4% CrO_3/SiO_2 catalyst.

The relationship between the reaction time and the catalytic activity per surface Cr atom, TON, at different CrO_3 contents is shown in Fig. 3. The TON decreases as a function of the reaction time and the chromium oxide content. The initial rates (20 min after the beginning of the reaction) possess a slightly higher TON than the steady state rates. The low chromium oxide content samples possess higher TON than the high chromium oxide content samples at all times. The color of the catalysts also varies with the reaction time and chromium content. The color of the catalysts changed from orange to brown and to light green at the initial state with increasing chromium oxide content and changed from light green to green at the steady state with increasing chromium oxide. This suggests that the formation of partially reduced chromium oxide species during the reaction and the high chromium oxide content samples possess more reduced chromium oxide species than the low chromium oxide content samples. The TON at steady state as a function of chromium oxide content is presented in Fig. 4. The TON decreases up to 1% CrO_3 and stays constant. A further increase in the chromium oxide content to 4% results in a slight decrease in the TON due to an increase in the concentration of crystalline α-Cr_2O_3. This result indicates that the surface chromium oxide species are more active than crystalline α-Cr_2O_3 for the methanol oxidation.

The product selectivity for the methanol oxidation reaction over CrO_3/SiO_2 catalysts is presented in Table 1 as a function of CrO_3 content. The main reaction product is formaldehyde (HCHO) regardless of chromium oxide content (selectivity in the range 54–76%), and methyl formate ($HCOOCH_3$), CO, and CO_2 are next in abundance. The

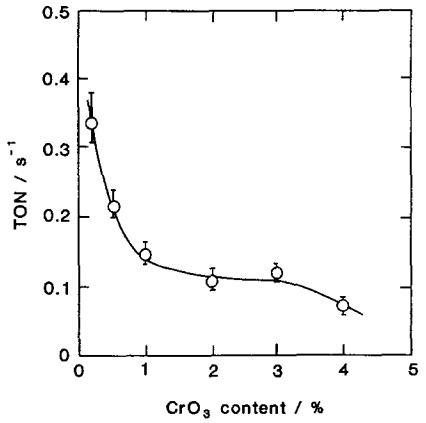

FIG. 4. TON for methanol oxidation at steady state over CrO_3/SiO_2 catalysts as a function of chromium oxide content.

TABLE 1

Selectivity for the Methanol Oxidation over CrO_3/SiO_2 Catalysts at Different CrO_3 Contents[a]

CrO_3 content (%)	Selectivity (%)					
	HCHO	$HCOOCH_3$	CO	CO_2	CH_3OCH_3	$(CH_3O)_2CH_2$
0.2(3.31×10^{-1})[b]	53.7	12.1	11.8	21.4	0.1	0.9
0.5(2.16×10^{-1})	53.6	13.9	11.9	19.0	0.4	1.2
1.0(1.39×10^{-1})	60.5	11.5	7.7	18.0	0.8	1.5
2.0(1.09×10^{-1})	70.7	9.1	5.1	13.3	0.9	0.9
3.0(1.14×10^{-1})	76.0	5.9	4.2	11.2	1.2	1.5
4.0(0.70×10^{-1})	72.9	8.0	5.2	10.3	1.8	1.8

[a] Reaction temperature is 503 K, $CH_3OH/O_2/He$=6/11/83 (mol %).
[b] Numbers in the parentheses are TON (s^{-1}) for the methanol oxidation at the steady state.

selectivity for dimethoxymethane ($(CH_3O)_2CH_2$) is less than 1.8%. The selectivity for dimethyl ether (CH_3OCH_3), which is produced by acidic sites on the catalysts (*29, 30*), is also below 1.8%. These products are minimal and can be neglected with respect to the other reaction products. The selectivity for HCHO increases as the chromium content increases, and the opposite trend is observed for the selectivity of $HCOOCH_3$, CO, and CO_2.

The effect of surface OH groups of silica on catalytic activity and selectivity has been reported (*24, 31*). McDaniel (*31*) has revealed that the catalytic activity for ethylene polymerization over CrO_3/SiO_2 is strongly dependent on the activation temperature (number of OH groups on silica surface). Che and co-workers (*24*) have also suggested that surface OH groups of silica are involved in the formation of $HCOOCH_3$. The number of surface hydroxyls on the silica support decreases with increasing chromium oxide content and calcination temperature: almost all the surface hydroxyls on silica are eliminated upon calcination of CrO_3/SiO_2 catalysts at 873–1073 K (*31*). To determine the influence of the silica support properties on the selectivity for methanol oxidation, the catalysts were also precalcined at 973 K for 3 h in the reactor to remove the surface hydroxyls on silica and the methanol oxidation reaction was conducted under the same reaction conditions. The results are summarized in Table 2. The Raman spectroscopic study showed that the silica support stabilizes the surface chromium(VI) oxide state and the surface structure of chromium oxide species under dehydrated conditions remained unchanged at elevated calcination temperature (973 K). In comparison with Table 1, the catalytic activity (TON) of the catalysts essentially remains unchanged, but the distribution of reaction products is drastically changed by the high-temperature precalcination treatment. It is interesting to note that the selectivity for HCHO is markedly increased, but the formation of $HCOOCH_3$ is significantly suppressed by the high-temperature precalcination treatment. A slight decrease in the selectivity for CO and CO_2 is also observed. Furthermore, the selectivity for HCHO also increases with increasing chromium oxide content (selectivity in the range 70–89%) and the selectivity for CO and CO_2 decreases.

The influence of reaction temperature on the selectivity of methanol oxidation over the 1% CrO_3/SiO_2 catalyst was also investigated and the results are presented in Table 3. The methanol oxidation selectivity is strongly dependent on the reaction temperature. The conversion as well as catalytic activity for methanol oxidation increases with increasing reaction temperature. In ad-

TABLE 2

Effect of Precalcination Temperature on Selectivity for the Methanol Oxidation over CrO_3/SiO_2 Catalysts[a]

CrO_3 content (%)	Selectivity (%)					
	HCHO	$HCOOCH_3$	CO	CO_2	CH_3OCH_3	$(CH_3O)_2CH_2$
0.2(2.88×10^{-1})[b]	70.1	—[c]	5.9	23.7	0	0.3
0.5(2.35×10^{-1})	75.3	2.2	4.9	16.0	0	1.6
1.0(1.35×10^{-1})	82.9	—[c]	3.5	12.7	0	0.9
2.0(0.92×10^{-1})	85.9	—[c]	2.5	10.6	0	1.0
3.0(1.19×10^{-1})	88.5	—[c]	1.6	8.7	0.3	0.9
4.0(0.85×10^{-1})	81.6	4.2	3.5	8.9	0.3	1.5

[a] The sample was precalcined in flowing O_2 at 973 K for 3 h; reaction temperature is 503 K, $CH_3OH/O_2/He$=6/11/83 (mol%).

[b] Numbers in the parentheses represent TON (s^{-1}) for the methanol oxidation at the steady state.

[c] Only a trace amount of $HCOOCH_3$ was observed.

dition, when the reaction temperature increases from 493 to 563 K, the selectivity for HCHO increases from 50.6 to 68.2%, but the selectivities for $HCOOCH_3$ and $(CH_3O)_2CH_2$ decrease from 24.4 to 2.0% and from 4.6 to 0.2%, respectively. These results indicate that the formation of HCHO is favorable at high reaction temperatures while the formation of $HCOOCH_3$ and $(CH_3O)_2CH_2$ is unfavorable at elevated temperatures. An increase in the selectivity for CO and CO_2 is observed at 583 K at the expense of a decrease in the HCHO selectivity.

DISCUSSION

The molecular structures of supported metal oxide catalysts are one of the least understood areas in heterogeneous catalysts. Recently, Deo and Wachs (*32*) have determined that the molecular structures of the hydrated surface metal oxide species (Re_2O_7, CrO_3 V_2O_5, MoO_3, etc.) on the oxide supports (TiO_2, ZrO_2, Al_2O_3, SiO_2, etc.) under ambient conditions are strongly dependent on the net pH at which the surface possesses zero surface charge. The net surface pH is determined by the specific oxide support and the surface coverage of the

TABLE 3

Selectivity for the Methanol Oxidation over 1% CrO_3/SiO_2 at Different Reaction Temperatures[a]

Reaction temp (K)	Selectivity (%)					
	HCHO	$HCOOCH_3$	CO	CO_2	CH_3OCH_3	$(CH_3O)_2CH_2$
493(8.51×10^{-2})[b]	50.6	24.4	5.0	15.0	0.4	4.6
503(1.39×10^{-1})	60.5	11.5	7.7	18.0	0.8	1.5
523(2.99×10^{-1})	62.8	7.3	12.1	17.1	0.3	0.4
543(3.61×10^{-1})	65.0	5.4	13.1	15.7	0.4	0.4
563(6.59×10^{-1})	68.2	2.0	13.1	16.1	0.4	0.2
583(1.11×10^{0})	58.6	0.4	16.8	23.9	0.3	0

Note. The conversion at 493, 503, 523, 543, 563, and 583 K is 3.7, 4.8, 12.8, 15.7, 28.6, and 48%, respectively.

[a] $CH_3OH/O_2/He$=6/11/83 (mol%).

[b] Numbers in parentheses represent TON (s^{-1}) for the methanol oxidation at the steady state.

metal oxide overlayer. Hardcastle and Wachs have discussed the surface structures of chromium oxide species on silica under hydrated conditions (*4*). According to them, the 0.2% CrO_3/SiO_2 catalyst possesses monomers, dimers, and trimers. As the chromium oxide content increases to 1%, trimers become the predominate species. Further increase in the chromium oxide content to 3–4% results in the formation of tetramers. The Raman spectra of surface chromium oxide species under hydrated conditions are very similar to those observed in aqueous solutions. Thus, the net pH at the point of zero charge is an important parameter in the regulation of the surface structures of the chromium oxide species under hydrated conditions. Upon dehydration, the Raman spectra of the surface chromium oxide species on silica are dramatically changed and only a single band due to the dehydrated chromium oxide species (986 cm^{-1}) on the silica surface is observed regardless of CrO_3 content. The absence of characteristic Raman features due to the bending mode of Cr–O–Cr linkage at 210–230 cm^{-1} over CrO_3/SiO_2 catalysts indicates that the surface chromium oxide species appears to be isolated on silica. The band observed at 986 cm^{-1} is assigned to the symmetric stretching mode of a highly distorted, tetrahedrally coordinated monochromate species on the silica support (*4*). The asymmetric stretching mode of monochromate species is not observed in the Raman spectra because of the weaker intensity of this band relative to the symmetric stretching mode and the strong background from the CrO_3/SiO_2 catalyst. Since the reference chromium oxide compounds show that the asymmetric mode precedes the symmetric mode in the Raman spectra (*33*), the asymmetric stretching vibrational mode of the dehydrated monochromate species should occur at a higher wavenumber than the symmetric stretching mode of the dehydrated monochromate species. The absence of Raman bands due to the hydrated surface chromium oxide species under dehydrated conditions indicates that the polymeric chromium oxide species (dimers, trimers, and tetramers) are not stable on the SiO_2 support under dehydrated conditions, and they convert to a highly distorted, isolated monochromate species. This suggests that the net pH at the point of zero charge is not important under dehydrated conditions because this concept is only applicable when water is present. As presented in Scheme 1, the water molecules on the silica surface are removed upon dehydration and the surface chromium species become bound to the silica surface through the oxygen bridge (Cr–O–Si). The shift in the Raman band position of the surface chromium oxide species upon dehydration to higher wavenumber, 900 to 986 cm^{-1}, are due to a different structure of the chromium oxide species. The dehydration/rehydration process is reversible so that exposure to water of the dehydrated CrO_3/SiO_2 sample results in the reappearance of hydrated chromium oxide species on the silica surface. Although the silica support has a high surface area (300 $m^2\ g^{-1}$), crystalline α-Cr_2O_3 particles are observed even at relatively low chromium oxide content ($\geq$2% CrO_3) compared to the other supports such as TiO_2, ZrO_2, and Al_2O_3. This is due to the low surface concentration of reactive hydroxyl groups on the silica support and their surface chemistry (*4, 6*).

During the methanol oxidation reaction water molecules are produced by oxidative dehydrogenation of methanol: $CH_3OH + \frac{1}{2}O_2 \rightarrow HCHO + H_2O$. Zecchina *et al.* (*34*) have discussed that the water adsorbed on α-Cr_2O_3 is removed upon degassing at 423–473 K. Recently, Chung *et al.* (*35*) have revealed that the amount of chemisorbed water decreased sharply and almost disappeared at 473 K in the presence of 3.6% methanol in oxygen over MoO_3 catalyst during an IR specroscopic study. In addition, they found that oxygen has a blocking effect for the chemisorption of water on the reduced MoO_3 sites. As shown in Scheme 1, the water molecules

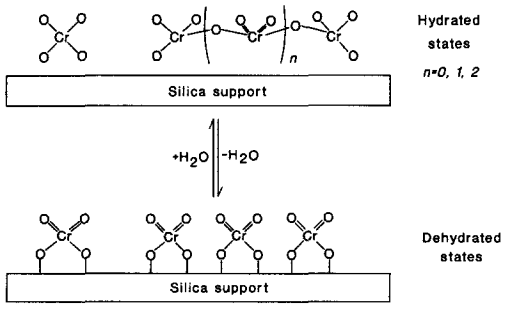

SCHEME 1. Two-dimensional model of surface chromium oxide species on the silica surface.

strongly influence the structure of the surface chromium oxide species. Therefore, the influence of water molecules produced during the methanol oxidation reaction on the structure of surface chromium oxide species has been investigated by Raman spectroscopy. The water vapor was introduced to the dehydrated CrO_3/SiO_2 catalyst in the stream of oxygen at 503 K for 0.5 h and then the spectrum was collected at room temperature. The result of Raman spectroscopic study shows that the water molecules do not affect the structure of the surface chromium oxide species at reaction temperature: no Raman band due to the hydrated chromium oxide species is observed in the spectrum. This result indicates that the reaction temperature used in this study (503 K) is higher than the desorption temperature of water molecules so that the desorption rate of water molecules is faster than the chemisorption rate of water molecules. Furthermore, the water molecules produced by methanol oxidation are not able to hydrolyze the bridging oxygen interacting with the support (Cr–O–Si) because the amount of water molecules produced by the reaction is small and the silica support is hydrophobic. These studies support the conclusion that the water molecules produced during the methanol oxidation reaction do not exert an affect on the surface structure of CrO_3/SiO_2 catalysts and that the dehydrated surface chromium oxide species remain unchanged by moisture. However, these species are partially reduced by the methanol molecules during the reaction.

As previously presented (see Fig. 2), the total methanol oxidation rate increases as the chromium oxide content increases to 3% CrO_3/SiO_2 and further increase in the chromium oxide content results in a slight decrease in the total rate. The decrease is due to the formation of crystalline α-Cr_2O_3, which is less active than the surface chromium oxide species. The increase in the total reaction rate as a function of the surface chromium oxide content indicates that the surface chromium oxide species are the catalytically active sites for the methanol oxidation. The TON of the reaction, assuming that all the chromium atoms are accessible to the reactants, decreases with the reaction time and the chromium oxide content (see Figs. 3 and 4). As stated previously, the color of catalysts also varies as a function of reaction time and chromium oxide content. The change in color of the catalysts suggests that some reduced chromium oxide species are formed during the methanol oxidation reaction. The orange and green colors are characteristic of Cr(VI) and Cr(III) species (*5*), respectively, and the brown color may be due to the mixture of Cr(VI) and Cr(III). Hogan (*9*) has determined the temperature at which reduction begins over SiO_2–Al_2O_3 supported metal oxide catalysts and concluded that supported CrO_3 catalysts reduce more readily than supported V_2O_5 or MoO_3 catalysts. The fact that the TON for the initial rates is higher than that of the steady state rates is attributed to the easier reducibility of the CrO_3/SiO_2 catalysts than the supported V_2O_5 and MoO_3 catalysts. The role of oxygen in the reactant is to reoxidize the reduced surface chromium oxide species that have been reduced by the methanol molecules during the reaction. However, the change in color as a function of the reaction time implies that the reoxidation by oxygen is somewhat slower than the reduction by methanol. The decrease in TON with increasing reaction time, with accompa-

nying change in color of the catalyst, indicates that the fully oxidized chromium oxide species are more active than the partially reduced chromium oxide species in the methanol oxidation reaction. The decrease in TON as a function of chromium oxide content regardless of precalcination temperature is attributed to the high reducibility of the high chromium oxide content samples.

The selectivity for HCHO increases as the chromium oxide content on SiO_2 increases and an opposite trend is observed for the selectivity of $HCOOCH_3$, CO, and CO_2 (see Table 1). High-temperature precalcination does not affect the TON but the selectivity is dramatically changed. The selectivity for HCHO increases by high-temperature precalcination (see Table 2). On the other hand, the selectivity for $HCOOCH_3$ is significantly retarded by high-temperature precalcination, whereas the selectivity for CO and CO_2 are slightly decreased. The results of these experiments strongly support the conclusion that the distribution of reaction products for methanol oxidation is strongly dependent on the number of surface hydroxyls on SiO_2 that depend on the chromium oxide content and precalcination temperature. A slight decrease in CO and CO_2 selectivity by high-temperature precalcination indicates that CO and CO_2 are produced not only on the silica site but also on the surface chromium oxide site.

The surface hydroxyls on silica are involved in the formation of $HCOOCH_3$ as revealed by the data presented in Tables 1 and 2. The surface hydroxyls on the silica support react readily with methanol and produce adsorbed CH_3O species (*36*). Thus, CH_3O species adsorbed on the silica surface participate in the formation of $HCOOCH_3$. Moreover, the selectivity for HCHO decreases as the chromium oxide content decreases (as the number of surface hydroxyls on silica increases) with an accompanying increase in the selectivity for $HCOOCH_3$. The results suggest that both HCHO species adsorbed on the chromium site and CH_3O species adsorbed on the silica site are involved in the formation of $HCOOCH_3$. Wachs and Madix (*37*) have proposed the reaction pathway for the formation of $HCOOCH_3$ over silver catalysts. Accordingly, $HCOOCH_3$ is produced via a H_2COOCH_3 (hemiacetal) intermediate, which is formed by the reaction between adsorbed HCHO and adsorbed CH_3O species. This kind of hemiacetal intermediate mechanism for the formation of $HCOOCH_3$ is also suggested by Takahashi *et al.*(*38*) over copper–silica catalysts. Recently, Che and co-workers (*24*) have proposed the reaction pathway for $HCOOCH_3$ formation over the MoO_3/SiO_2 catalysts prepared by the grafting method. According to this mechanism, $HCOOCH_3$ is produced by the hemiacetal intermediates that are formed by the spillover of adsorbed HCHO species initially formed on the Mo sites to the silica sites which further react with neighboring CH_3O species adsorbed on silica. On the basis of the obtained results and the reaction pathway stated previously, it can be concluded that over CrO_3/SiO_2 catalyst, $HCOOCH_3$ is produced via hemiacetal intermediates formed by the interaction between HCHO adsorbed on the Cr site and CH_3O adsorbed on an adjacent silica site.

The interaction between the adsorbed HCHO and CH_3O species is also observed during the formation of $HCOOCH_3$ in the Tischenko reaction (*39, 40*), $2H_2CO + Al(OCH_3)_3 \rightarrow HCOOCH_3$. The Tischenko mechanism initiates the transformation of alkoxide agent to an aldehyde. Similarly, over the CrO_3/SiO_3 catalysts, the CH_3O adsorbed on the silica surface attacks HCHO adsorbed on the Cr site and produces the hemiacetal intermediates, which subsequently yield $HCOOCH_3$ and hydrogen. As shown in Table 1, the selectivity for HCHO increases with chromium oxide content (i.e., increases as an inverse function of free surface hydroxyls on the silica support). The opposite trend is observed for the selectivity of $HCOOCH_3$. As the number of surface hydroxyls on the silica surface decreases, the number of CH_3O species

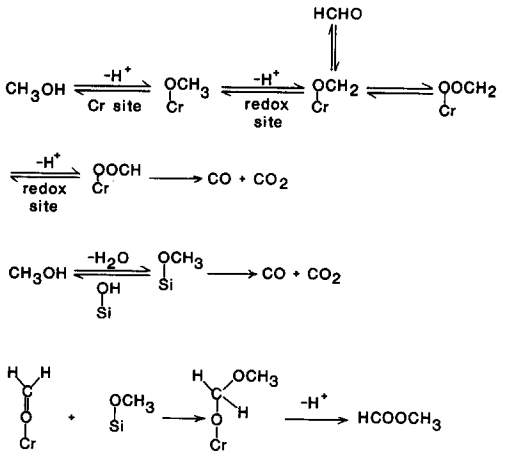

SCHEME 2. Proposed reaction pathway of methanol oxidation over CrO_3/SiO_2 catalysts.

adsorbed on the silica surface also decrease. Therefore, HCHO species adsorbed on the Cr site are less likely to interact with CH_3O species adsorbed on silica, and those species are readily desorbed and lead to an increase in HCHO selectivity. As expected, the selectivity for HCHO is enhanced when the surface hydroxyls on silica are removed by high-temperature precalcination (see Table 2). On the other hand, as the number of the surface hydroxyls on silica increases, the adsorbed HCHO species have a greater chance to interact with CH_3O species adsorbed on silica, so that the selectivity for $HCOOCH_3$ increases at the expense of the selectivity for HCHO. The obtained results indicate that HCHO and $HCOOCH_3$ are produced on the two different active sites: HCHO is produced by the desorption of adsorbed HCHO produced on the Cr sites and $HCOOCH_3$ is formed via hemiacetal intermediates produced by the interaction between adsorbed HCHO formed on the Cr site and CH_3O adsorbed on the silica site. CO and CO_2 are produced on both the Cr and silica sites.

A reaction pathway for methanol oxidation over CrO_3/SiO_2 catalysts is proposed and shown in Scheme 2. The primary step in the oxidation of methanol is the dissociative adsorption of methanol on the Cr site, which results in the formation of adsorbed CH_3O and hydroxyls. It is well established that the adsorbed CH_3O groups are easily produced on supported (*30, 41*) and unsupported metal oxides (*36, 42*), even at room temperature. Abstraction of an H-atom from the adsorbed CH_3O groups by an adjacent oxygen results in the formation of adsorbed HCHO intermediates. Isotopic studies revealed that this step is the rate-determining step in methanol oxidation over molybdenum oxide catalysts (*43, 44*). Desorption of adsorbed HCHO species produces the gaseous HCHO and this step is effectively facilitated when the number of surface hydroxyls on the silica decreases and the reaction temperature increases. On the other hand, the reaction of methanol with the surface hydroxyls on silica results in the formation of adsorbed CH_3O species (*36*). The adsorbed CH_3O species present on the silica surface interact with adsorbed HCHO on the Cr sites and this leads to the formation of $HCOOCH_3$ via hemiacetal intermediates at the expense of HCHO selectivity. Wachs and Madix (*37*) have provided the evidence that the abstraction of the H-atom from hemiacetal intermediates is the rate-determining step for the formation of $HCOOCH_3$ over the silver catalyst by performing an isotopic study. Tables 1 and 2 suggest that CO and CO_2 combustion products are produced at both the Cr and the silica sites. The decomposition of CH_3O species adsorbed on silica results in the formation of these products. Moreover, Busca *et al.* (*45*) and Wachs and Madix (*37*) have proposed that CO and CO_2 are produced via formate ions (HCOO). Similarly, HCHO adsorbed on the Cr sites is further oxidized to adsorbed H_2COO species. These intermediates are unstable so they yield HCOO species, and decomposition of HCOO species results in the formation of CO and CO_2 (*37*).

It is interesting to compare the current findings for methanol oxidation over silica-supported chromium oxide catalysts with

corresponding studies with ethylene polymerization over silica-supported chromium oxide catalysts. Silica-supported chromium oxide catalysts need to be activated by a high-temperature calcination of 573 to 1273 K in order to be active for ethylene polymerization (*9, 31*). The present study reveals that this treatment is necessary to remove the adsorbed moisture, which coordinated to the surface chromium oxide and alters its structure. In the presence of adsorbed moisture, the surface chromium oxide species on silica is present as a polymerized chromium oxide species and all Cr–O–Si bonds are hydrolyzed. The high-temperature calcination removes the adsorbed moisture and hydrated polymerized chromium oxide species decomposes and anchors to the silica support by forming Cr–O–Si bonds. The dehydrated surface chromium oxide species is monochromate and possesses tetrahedral coordination with two terminal Cr=O bonds (dioxo). Only on the silica support is a dehydrated monochromate species formed, but on all other oxide supports (alumina, titania, zirconia, and niobia) a dehydrated polymerized chromium oxide species is also present (*46*). Thus, the calcination treatment is critical to forming the dehydrated surface chromium oxide species, which is the active precursor to ethylene polymerization.

The total rates of methanol oxidation (mmol g^{-1} h^{-1}) and ethylene polymerization (g polyethylene/g catalyst) are directly related to surface monochromate content. The total rate of methanol oxidation increases to approximately 3% CrO_3 content, which according to the Raman characterization studies corresponds to the maximum amount of surface monochromate species on silica (see Fig. 2). Higher chromium oxide contents result in significant crystalline Cr_2O_3 formation, which has an adverse effect on the total reaction rate of the catalyst. An identical reactivity pattern was obtained when these catalysts were examined for ethylene polymerization (*47*) and also previously reported in the literature (*9*). Another similarity between these two reactions is that the TON, reactivity per chromia atom, decreased with increasing chromium oxide content as the amount of chromium oxide is increased to 3% CrO_3 content. This decrease in TON with decreasing chromium oxide content is not fully understood at present. These comparative studies, however, demonstrate that the reactivity of both reactions are directly related to the surface monochromate species.

Furthermore, the activation temperature of the silica-supported chromium oxide catalysts also has a significant effect on both reactions. For methanol oxidation, higher activation temperatures decrease the selectivity toward $HCOOCH_3$ formation. For ethylene polymerization, higher activation temperatures increase the catalytic activity for polymerization. Both of these events are related to the decrease in surface hydroxyls on the silica surface at elevated temperatures since the surface hydroxyls are involved in the formation of $HCOOCH_3$ and apparently retard the ethylene polymerization reaction. Increasing the surface monochromate content has the same effect since it also decreases the surface hydroxyl concentration.

The parallel behavior of the silica-supported chromium oxide catalysts for the methanol oxidation and ethylene polymerization reactions reveals that the same surface chromium oxide precursor is involved in both reactions. This common precursor is the surface monochromate species that is present in the Cr(VI) oxidation state in the activated state. However, during methanol oxidation the surface chromia oxidation state is only moderately decreased relatively to the more extensively reduced Cr(III) and/or Cr(II) that is present during ethylene polymerization (*9, 31*). The similar reactivity patterns of silica-supported chromium oxide for both reactions, net reducing and mixed reducing/oxidizing, under very different environments, suggests that the catalyst reactivity is prede-

termined by the oxidic state of the catalyst and not the specific reactant molecule or the reaction environment (reducing vs oxidizing). This further suggests that methanol oxidation may be used as a simple probe reaction to determine the reactivity of silica-supported chromium oxide catalysts that are typically used for ethylene polymerization.

CONCLUSIONS

The molecular structures of two-dimensional chromium oxide overlayers on the silica surface were determined using *in situ* Raman spectroscopy. The surface chromium oxide species on the silica surface under dehydrated conditions possess the highly distorted monochromate species regardless of chromium oxide content. The crystalline α-Cr_2O_3 phase is also observed at the 2% CrO_3/SiO_2 catalyst and increases with further increase in the chromium oxide content. Catalysts possessing a low content of chromium oxide exhibit higher TON for methanol oxidation but are less selective toward HCHO than catalysts containing a high content of chromium oxide. The slight decrease in TON as a function of reaction time, which correlates with the change in color of the catalysts, indicates that the fully oxidized chromium oxide species (Cr(VI)) are more active for methanol oxidation than the reduced chromium oxide species. The main product during methanol oxidation is HCHO regardless of chromium oxide content, and $HCOOCH_3$, CO, and CO_2 are next in abundance. The selectivity for HCHO increases with chromium oxide content and high-temperature precalcination. The opposite trend is observed for the selectivity of $HCOOCH_3$. These results suggest that the number of surface hydroxyls on silica exerts an affect on the distribution of reaction products during methanol oxidation. HCHO is formed on the Cr site, whereas $HCOOCH_3$ is produced via hemiacetal intermediates, which are formed by interaction between HCHO adsorbed on the Cr site and CH_3O adsorbed on the silica site. CO and CO_2 are produced on both the chromium and the silica sites.

REFERENCES

1. Richter, M., Reich, P., and Ohlmann, G., *J. Mol. Catal.* **46,** 79 (1988).
2. Zaki, M. I., Fouad, N. E., Leyrer, J., and Knozinger, H., *Appl. Catal.* **21,** 359 (1986).
3. Fubini, B., Ghiotti, G., Stradella, L., Garrone, E., and Morterra, C., *J. Catal.* **66,** 200 (1980).
4. Hardcastle, F. D., and Wachs, I. E., *J. Mol. Catal.* **46,** 173 (1988).
5. Groeneveld, C., Wittgen, P. P. M. M., Van Kersbergen, A. M., Mestrom, P. L. M., Nuijiten, C. E., and Schuit, G. C. A., *J. Catal.* **59,** 153 (1979).
6. Merryfield, R., McDaniel, M. P., and Parks, G., *J. Catal.* **77,** 348 (1982); McDaniel, M. P., and Johnson, M. M., *J. Catal.* **101,** 446 (1986).
7. Ellison, A., *J. Chem. Soc. Faraday Trans. 1* **80,** 2567 (1984).
8. Krauss, H. L., *in* "Proceedings, 5th International Congress on Catalysis, Palm Beach, 1972" (J. W. Hightower Ed.), Vol. 1, p. 207. North-Holland, Amsterdam, 1973.
9. Hogan, J. P., *in* "Applied Industrial Catalysis" (B. E. Leach, Ed.). Academic Press, New York, 1983; *J. Polym. Sci.* **8,** 2637 (1970).
10. Hogan, J. P., and Bank, R. L., Belg. Pat., 530 617 (January 24, 1985); US Pat., 2 825 721 (March 4, 1958).
11. Beck, D. D., and Lunsford, J. H., *J. Catal.* **68,** 121 (1981).
12. Richter, M., and Ohlmann, G., *React. Kinet. Catal. Lett.* **29,** 211 (1985).
13. Parlitz, B., Hanke, W., Fricke, R., Richter, M., Roost, U., and Ohlmann, G., *J. Catal.* **94,** 24 (1985).
14. Baes, C. F., Jr., and Mesmer, R. E., "The Hydrolysis of Cations." Wiley, New York, 1986.
15. Michel, G., and Machiroux, R., *J. Raman Spectrosc.* **14,** 22 (1983); *17,* 79 (1986).
16. Vuurman, M. A., Stufkens, D. J., Oskam, O., Moulijn, J. A., and Kapteijn, F., *J. Mol. Catal.* **60,** 83 (1990).
17. Michel, G., and Cahay, R., *J. Raman Spectrosc.* **17,** 4 (1986).
18. Tatibouet, J. M., Che, M., Amirouche, M., Fournier, M., and Rocchiccioli-Deltcheff, C., *J. Chem. Soc. Chem. Commun.,* 1260 (1988).
19. Volta, J. C., and Portefaix, J. L., *Appl. Catal.* **18,** 1 (1985).
20. Tatibouet, J. M., Germain, J. E., and Volta, J. C., *J. Catal.* **82,** 240 (1983).
21. Tatibouet, J. M., and Germain, J. M., *J. Catal.* **72,** 375 (1981).
22. Ohuchi, F., Firment, L. E., Chowdhry, U., and Ferretti, A., *J. Vac. Sci. Technol., A* **2,** 1022 (1984).

23. Segawa, K., Soeya, T., and Kim, D.S., *Sekiyu Gakkaishi* **33,** 347 (1990).
24. Louis, C., Tatibouet, J. M., and Che, M., *J. Catal.* **109,** 354 (1988).
25. Haber, J., Kozlowska, A., and Kozlowski, R., *J. Catal.* **102,** 52 (1986).
26. Roozeboom, F., Cordingleys, P. D., and Gellings, P. J., *J. Catal.* **68,** 464 (1981).
27. Deo, G., and Wachs, I. E., *J. Catal.* **129,** 307 (1991).
28. Wang, L., Ph.D. thesis, University of Wisconsin, 1982.
29. Jehng, J. M., and Wachs, I. E., *Catal. Today* **8,** 37 (1990).
30. Kim, D. S., Ph.D. thesis, Sophia University, Tokyo, 1990.
31. McDaniel, M. P., *J. Catal.* **67,** *71 (1981);* **76,** 17, 29, and 37 (1982).
32. Deo, G., and Wachs, I. E., *J. Phys. Chem.* **95,** 5889 (1991).
33. Matters, R., *Z. Anorg. Allg. Chem.* **382,** 163 (1971).
34. Zecchina, A., Coluccia, S., Guglielminotti, E., and Ghiotti, G., *J. Phys. Chem.* **75,** 2774 (1971).
35. Chung, J. S., Miranda, R., and Bennett, C. O., *J. Chem. Soc. Faraday Trans. 1* **81,** 19 (1985).
36. Morrow, B. A., *J. Chem. Soc. Faraday Trans. 1* **70,** 1527 (1974).
37. Wachs, I. E., and Madix, R. J., *Surf. Sci.* **76,** 531 (1978).
38. Takahashi, K., Takazawa, N., and Kobayashi, H., *Chem. Lett.,* 1061 (1983).
39. Ogata, Y., Kawasaki, A., and Kishi, I., *Tetrahedron* **23,** 825 (1967); Ogata, Y., and Kawasaki, *Tetrahedron* **25,** 929 (1969).
40. Saegusa, T., Ueshima, T., and Kitakawa, S., *Bull. Chem. Soc. Jpn.* **42,** 248 (1969).
41. Busca, G., *J. Mol. Catal.* **50,** 241 (1989).
42. Busca, G., and Loenzelli, V., *J. Catal.* **66,** 155 (1980).
43. Yang, T. J., and Lunsford, J. H., *J. Catal.* **103,** 55 (1987).
44. Machiels, C. J., and Sleight, A. W., *J. Catal.* **76,** 238 (1982).
45. Busca, G., Elmi, A. S., and Forzatti, P., *J. Phys. Chem.* **91,** 5263 (1987).
46. Vuurman, M. A., Wachs, I. E., Stufken, D. J., and Oskam, O., manuscript submittied.
47. Brant, P., and Wachs, I. E., unpublished work.